Developmental Biology 371 (2012) 136–145

Contents lists available at SciVerse ScienceDirect

Developmental Biology

journal homepage: www.elsevier.com/locate/developmentalbiology

EpCAM contributes to formation of functional tight junction in the intestinal epithelium by recruiting claudin proteins

Zili Lei [a,b,1], Takako Maeda [a,b,1], Atsushi Tamura [c,1], Tetsuya Nakamura [a,b], Yuji Yamazaki [c], Hidetaka Shiratori [a,b], Kenta Yashiro [a,b], Sachiko Tsukita [c,*], Hiroshi Hamada [a,b,**]

[a] Developmental Genetics Group, Graduate School of Frontier Biosciences, Osaka University, 1-3 Yamada-oka, Suita, Osaka 565-0871, Japan
[b] CREST, Japan Science and Technology Corporation (JST), 1-3 Yamada-oka, Suita, Osaka 565-0871, Japan
[c] Laboratory of Biological Science, Graduate School of Frontier Biosciences and Graduate School of Medicine, Osaka University, 2-2 Yamada-oka, Suita, Osaka 565-0871, Japan

ARTICLE INFO

Article history:
Received 7 February 2012
Received in revised form
6 July 2012
Accepted 8 July 2012
Available online 20 July 2012

Keywords:
Claudin
Epithelial barrier
Intestine
Tight junction

ABSTRACT

Tight junctions (TJs) connect epithelial cells and form a semipermeable barrier that only allows selective passage of ions and solutes across epithelia. Here we show that mice lacking EpCAM, a putative cell adhesion protein frequently overexpressed in human cancers, manifest intestinal barrier defects and die shortly after birth as a result of intestinal erosion. EpCAM was found to be highly expressed in the developing intestinal epithelium of wild-type mice and to localize to cell–cell junctions including TJs. Claudin-7 colocalized with EpCAM at cell–cell junctions, and the two proteins were found to associate with each other. Claudins 2, 3, 7, and 15 were down-regulated in the intestine of EpCAM mutant mice, with claudin-7 being reduced to undetectable levels. TJs in the mutant intestinal epithelium were morphologically abnormal with the network of TJ strands scattered and dispersed. Finally, the barrier function of the intestinal epithelium was impaired in the mutant animals. These results suggest that EpCAM contributes to formation of intestinal barrier by recruiting claudins to cell–cell junctions.

Introduction

During our search for pluripotency-associated genes in embryonal carcinoma cell lines (Saijoh et al., 1996), we identified *EpCAM* as a gene that is specifically expressed in undifferentiated cells. Previous studies have revealed that EpCAM contributes to various biological processes including cell signaling, migration, and proliferation (de Boer et al., 1999; Litvinov et al., 1997; Maghzal et al., 2010). EpCAM was originally identified as a tumor-associated antigen on the basis of its high level of expression in rapidly growing tumors of epithelial origin (Trzpis et al., 2007). EpCAM-positive cells have been suggested to serve as cancer stem cells for various human cancers including colorectal and hepatocellular carcinoma (Dalerba et al., 2007; Yamashita et al., 2009). A proteolytic fragment of EpCAM containing the intracellular domain was recently shown to form a complex with β-catenin and Lef-1 that translocates to the nucleus and activates the transcription of genes related to cell proliferation, such as those for c-Myc and cyclins A and E, and thereby to promote oncogenesis (Maetzel et al., 2009). EpCAM is also implicated in maintenance of pluripotency in embryonic stem cells (Gonzalez et al., 2009; Lu et al., 2010) as well as in somatic stem cells such as hepatic stem cells (Okabe et al., 2009; Schmelzer et al., 2006; Schmelzer et al., 2007; Tanaka et al., 2009).

EpCAM (CD326, also known as Tacstd1), a type I transmembrane glycoprotein that contains two EGF-like domains, a single transmembrane domain, and a small intra cellular domain (Winter et al., 2003), has been implicated in homotypic cell–cell adhesion in epithelia (Litvinov et al., 1994), but its precise role in epithelial cell adhesion remains unclear. A recent study of zebrafish lacking EpCAM suggested that this protein functions as a partner of E-cadherin in epithelial morphogenesis during epiboly and skin development (Slanchev et al., 2009). Adhesive structures between adjacent cells, including tight junctions (TJs) and adherens junctions (AJs), are not only required for tissue integrity but also act as signaling structures. While adhesion at AJs is mediated by cadherins, a conserved family of adhesion molecules, TJs contain many adhesive molecules including claudins, occludin, ZO-1 and junctional adhesion molecules (JAMs) (Tsukita et al., 2001).

Although EpCAM is implicated in various biological events, its physiological function remains unclear. To investigate the function of EpCAM in vivo, we generated two EpCAM knockout mouse

* Corresponding author.
** Corresponding author at: Developmental Genetics Group, Graduate School of Frontier Biosciences, Osaka University, 1-3 Yamada-oka, Suita, Osaka 565-0871, Japan. Fax: +81 6 6878 9846.
E-mail addresses: atsukita@biosci.med.osaka-u.ac.jp (S. Tsukita), hamada@fbs.osaka-u.ac.jp (H. Hamada).
[1] These authors contributed equally to this work.

0012-1606/$ - see front matter © 2012 Published by Elsevier Inc.
http://dx.doi.org/10.1016/j.ydbio.2012.07.005

models by gene targeting. We now show that EpCAM contributes to formation of functional TJs in the intestinal epithelium by recruiting claudin proteins to apical cell–cell junctions.

Materials and methods

Mice

Two mutant alleles of the EpCAM gene were generated by gene targeting in embryonic stem cells (Fig. S2): the *EpCAM*$^{\beta geo}$ allele, in which a βgeo cassette and a loxP site are inserted into intron 1 and another loxP site is inserted into intron 3; and the *EpCAM*$^{-}$ allele, in which exons 2 and 3 are deleted. Both mutant alleles are functionally null. Heterozygous mutant mice were maintained on the 129/C57B6 mixed background. All experiments were approved by the Institutional Animal Care and Use Committee of the Osaka University.

Histological analysis and immunostaining

For histological analysis, tissue was fixed overnight at 4 °C in PBS containing 4% paraformaldehyde, dehydrated, embedded in paraffin, sectioned, and stained with hematoxylin–eosin. Alcian blue staining was performed according to standard protocols. Frozen sections were stained for 30 min at room temperature with 1% AB 8GX (Sigma) in 3% acetic acid, and then counterstained with nuclear fast red. For X-gal staining, frozen sections were stained overnight at 37 °C with a pH 7.3 solution containing 2 mM $MgCl_2$, 4 mM potassium ferricyanide, 4 mM potassium ferrocyanide and 0.1% X-gal in PBS. For alkaline phosphatase staining, the sections were stained for 30 min at room temperature with NBT/BCIP (Roche) in 100 mM NaCl, 100 mM Tris–HCl (pH9.5), 50 mM $MgCl_2$ and 0.1% Tween20. For immunostaining, frozen sections (thickness of 7 μm) were exposed to 1% BSA in PBS containing 0.1% Tween-20 to block nonspecific sites before incubation first overnight at 4 °C with primary antibodies and then for 1 h at room temperature with secondary antibodies. Primary antibodies included rat anti-Ki67 (1:1500 dilution, M724901) from DakoCytomation; mouse anti-c-Myc (1:200, sc-40) and goat anti-EpCAM (1:200, sc-23788) from Santa Cruz Biotechnology; rabbit anti-claudin-7 (1:1000, #34-9100) from Zymed; rabbit anti-claudin-15 (1:250, #38–9200), mouse anti–claudin-2 (1:250, #32-5600), rabbit anti-claudin-3 (1:200, #34-1700), and mouse anti-plakoglobin (1:300, #138500) from Invitrogen; rat anti-occludin, rat anti-ZO-1, and rat anti-E-cadherin generated in-house; rabbit anti-cleaved caspase3 (1:100, #9661) from Cell signaling and rabbit anti-EpCAM (1:1000, ab32392) from Abcam. Immunofluorescence analysis was performed with Alex Fluor 488- or Alexa Fluor 568-labeled secondary antibodies (Invitrogen), whereas immunohistochemical analysis was performed with biotin-conjugated secondary antibodies (Jackson laboratory), HRP-ABC complex (VECTASTAIN) and DAB (DOJINDO). Use Zeiss or Olympus confocal microscope to observe the immunofluorescence sections, and immunohistochemical photos were got by using Nikon microscope and Olympus camera.

In situ hybridization

The intestine was fixed overnight at 4 °C with 4% paraformaldehyde in PBS, dehydrated, embedded in OCT compound, and sectioned at a thickness of 7 μm. The sections were fixed again with 4% paraformaldehyde in PBS, treated with 0.2 M HCl, digested with proteinase K, re-fixed with 4% paraformaldehyde in PBS, treated with 0.25% acetic anhydride, and subjected to hybridization for 24–48 h at 55 °C with specific digoxigenin-labeled probes in 5 × SSC (pH 5.0) containing 50% formamide, 1% SDS, yeast tRNA (50 μg/ml), and heparin (50 μg/ml). Sections were then washed at 55 °C shortly first with 5 × SSC and then with 2 × SSC containing 50% formamide for 15 min before incubation for 30 min at 37 °C with RNase A (10 μg/ml; Sigma) in TNE buffer [10 mM Tris–HCl (pH 8.0), 500 mM NaCl, 1 mM EDTA]. After washing twice for 20 min with 2 × SSC and then twice for 20 min with 0.2 × SSC at 50 °C, the sections were incubated at room temperature first for 5 min in TBS containing 0.1% Tween 20 and then for 1 h in the same solution containing 1% blocking powder (Roche). They were subsequently incubated overnight at 4 °C with the blocking solution containing alkaline phosphatase–conjugated antibodies to digoxigenin (1:2000 dilution; Roche). After several washes with TBS containing 0.1% Tween 20, immune complexes were detected with NBT/BCIP solution (Roche). The sections were finally dehydrated with a graded series of ethanol solutions and permanently mounted on glass slides. Microscopic analysis was performed as described for immunostaining. Whole-mount in situ hybridization was performed according to standard protocols (Wilkinson, 1992).

Immunoprecipitation and immunoblot analysis

The entire intestine of E18.5 embryos was homogenized by hand for 1 h on ice in lysis buffer [25 mM Hepes–NaOH (pH 7.2), 150 mM NaCl, 5 mM $MgCl_2$] containing 1% CHAPS (Kuhn et al., 2007) as well as a protease inhibitor cocktail (Roche) and 2 mM PMSF. The homogenate was centrifuged at 17,600*g* for 10 min at 4 °C, and the resulting supernatant (1 ml) was incubated for 2 h at 4 °C with 1/10 volume of protein G-Sepharose (GE Healthcare) and protease inhibitor cocktail. After removal of the resin by centrifugation, the tissue lysate was incubated overnight at 4 °C with 3 μg of specific antibodies or control IgG, with protein G-Sepharose being added for the final 4 h. The resin was then isolated by centrifugation, washed six times with lysis buffer, and subjected to SDS-PAGE on a 12% or 15% gel. The separated proteins were transferred electrophoretically to a polyvinylidene difluoride membrane overnight at 30–40 V and 4 °C, after which the membrane was exposed to a solution containing 3% nonfat milk powder and 0.1% Tween 20 before immunoblot analysis with primary antibodies and ECL Plus reagents (Amersham). Primary antibodies included goat anti-EpCAM (1:25 dilution; sc-23788,Santa Cruz Biotechnology), rabbit anti-claudin-7 (1:5000; #34-9100, Zymed), rabbit anti-claudin-3 (1:500; #34-1700, Invitrogen), mouse anti-claudin-2 (1:500; #32-5600, Invitrogen), and rabbit anti-claudin-15 (1:250; #38-9200, Invitrogen).

Electron microscopy

The jejunum was excised from mouse pups at P1, washed gently with 0.1 M Hepes–NaOH (pH 7.3), cut into small pieces, and processed for ultrathin-section electron microscopy according to standard protocols. For freeze-fracture electron microscopy, the P1 jejunum was fixed for 1 h at room temperature with 2% glutaraldehyde in 0.1 M Hepes–NaOH (pH 7.3), washed three times with the Hepes buffer alone, immersed for 2 h in the Hepes buffer containing 30% glycerol, and then frozen in liquid nitrogen. The frozen samples were fractured at –110 °C with freeze-etching equipment (EM-19500NFSDT, JEOL). All samples were observed with a JEM1010 (JEOL) electron microscope at an acceleration voltage of 100 kV.

Barrier function assays

The barrier function assay based on sulfo-NHS-biotin was performed as described previously (Tamura et al., 2008). In brief,

E18.5 embryos were dissected from the uterus, after which the abdominal cavity was opened. A 30-gauge needle was inserted into the upper portion of the duodenum near the junction with the stomach, and ~0.2 ml of sulfo-NHS-biotin (1 mg/ml; Sigma) was injected into the lumen of the intestine. The embryos were incubated in a humidified chamber for 30 min at room temperature, after which the small intestine was cut into four pieces. The tissue was washed in PBS for ~5 min, fixed overnight at 4 °C with 4% paraformaldehyde in PBS, dehydrated, embedded in OCT compound, and sectioned. The sections were incubated for 1 h at room temperature with a 1:500 dilution of Alexa Fluor 488-conjugated streptavidin (Invitrogen) and then processed for fluorescence microscopy. For assay of Lucifer yellow flux, jejunal sheets were excised from P3.5 pups and mounted in a dual-channel Ussing chamber (opening of 0.0314 cm^2 between the two halves of the chamber). Each side of the chamber was filled with 3 ml of a solution containing 120 mM NaCl, 10 mM Hepes–NaOH (pH 7.4), 5 mM KCl, 10 mM $NaHCO_3$, 1.2 mM $CaCl_2$, and 1 mM $MgSO_4$. Lucifer yellow (457.25 Da; Nacalai Tesque) was added to the serosal/mucosal side of the chamber at a final concentration of 0.5 mg/ml. After incubation of the chamber for 60 min at 37 °C, tissue permeability was determined by removal of the medium from the mucosal/serosal side of the chamber not initially containing Lucifer yellow for measurement of dye fluorescence with a microplate fluorescence reader.

Culture of duodenum explants with MG132

WT or *EpCAM*$^{-/-}$ duodenums were excised from E18.5 embryo. Immediately after dissection, duodenum explants were cultured in 50% Rat Serum and 50% DMEM medium with or without MG132 (10 μg/ml) for 24 h. After 24 h, duodenum explants were fixed by 4% PFA and were stained for claudin-7.

Results

EpCAM mutant mice exhibit intestinal defects

We previously searched for pluripotency-associated genes in the mouse P19 embryonal carcinoma cell line and its derivatives (Saijoh et al., 1996), and we found that *EpCAM* is expressed at a high level in undifferentiated P19 cells but is down-regulated in differentiated P19 cells (Fig. S1A) (Shimazaki et al., 1993). In the developing mouse embryo, *EpCAM* is expressed specifically in the inner cell mass of the blastocyst, in the epiblast at embryonic day (E) 5.5 and E6.5, and in the developing gonads at E12.5 (Fig. S1B). This expression pattern is similar to that of *Oct3/4* (Saijoh et al., 1996; Scholer et al., 1990), a functional marker of pluripotency.

To determine the physiological function of EpCAM, we generated mice deficient in this protein. Two types of mutant allele were generated: *EpCAM*$^{-}$ and *EpCAM*$^{\beta geo}$ (Fig. S2). The phenotypes of *EpCAM*$^{-/-}$ and *EpCAM*$^{\beta geo/\beta geo}$ mice were indistinguishable, suggesting that both alleles are null. In fact, EpCAM protein was not detected in the intestine of *EpCAM*$^{-/-}$ or *EpCAM*$^{\beta geo/\beta geo}$ mice (Fig. S3A and B). Examination of newborn offspring of heterozygote intercrosses revealed that the frequency of homozygous mutant mice was slightly smaller than expected (22.43% for *EpCAM*$^{-/-}$ and 13.76% for *EpCAM*$^{\beta geo/\beta geo}$) (Table S1), suggesting that the mutant alleles are embryonic lethal in a small proportion of mutant homozygotes. A previous study found that *EpCAM* mutant mice die during embryogenesis as a result of impaired development of the placenta (Nagao et al., 2009). The homozygous mutant mice in the present study had a body size similar to that of wild-type (WT) mice at birth and were able to take milk from the mother. However, the mutant mice had diarrhea and did not gain body weight, with most dying within 10 days after birth (Fig. S4). Examination of abdominal organs revealed that the intestine was most prominently affected in the mutant animals. At the newborn stage [postnatal day (P) 0 to P1], the intestine of the mutant mice appeared relatively normal both macroscopically (Fig. 1A) and histologically (Fig. S5). At P4, however, bleeding was apparent within the mutant intestine, rendering it brown in color (data not shown). At P6, severe intestinal bleeding and obstruction were evident in the mutant mice (Fig. 1A). Perforation was also observed at many sites of the mutant intestine. Histological analysis revealed disruption of mucosal architecture and sloughing epithelial cells in the mutant intestine at P5, which were more

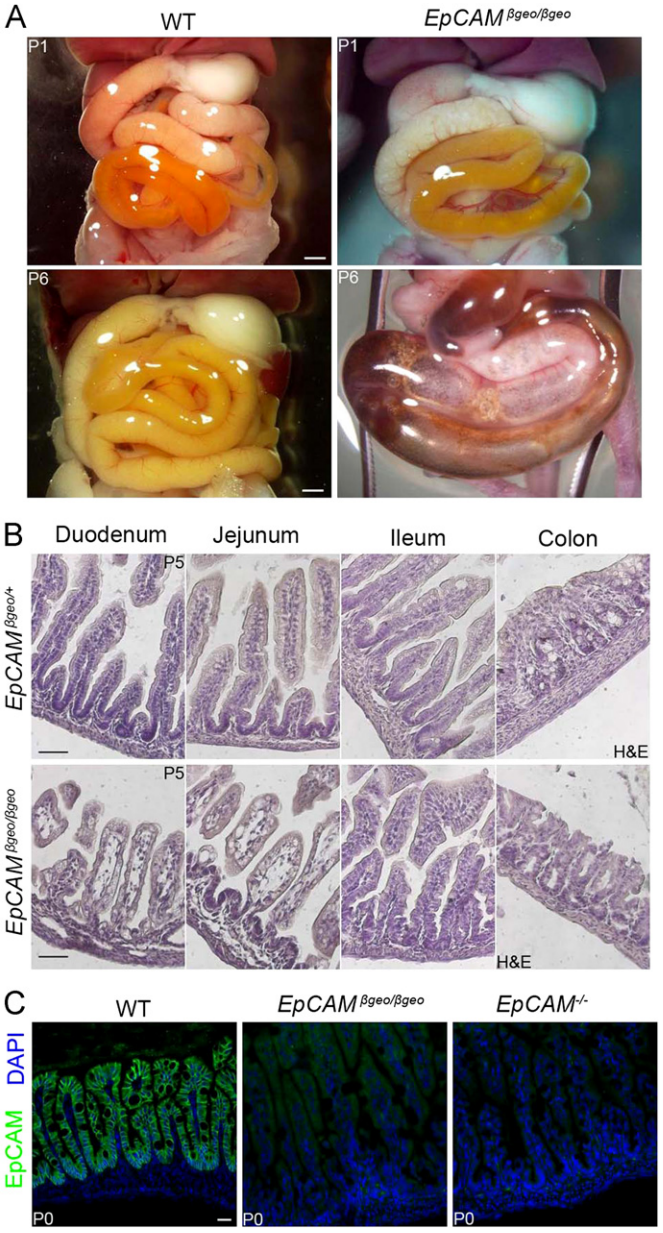

Fig. 1. Intestinal defects in EpCAM mutant mice: (A) macroscopic morphology of the intestine of WT and *EpCAM*$^{\beta geo/\beta geo}$ mouse pups at P1 and P6. The mutant intestine appears normal at P1, but severe intestinal bleeding is evident at P6. Bars, 1 mm. (B) Hematoxylin–eosin (H&E) staining of the intestine of *EpCAM*$^{\beta geo/+}$ and *EpCAM*$^{\beta geo/\beta geo}$ mice at P5. The morphology of the duodenum and jejunum of the mutant pups was abnormal, with the subepithelial regions of these segments being devoid of content, whereas the ileum and colon remained normal. Bars, 50 μm. (C) Frozen sections of the small intestine of WT, *EpCAM*$^{\beta geo/\beta geo}$, or *EpCAM*$^{-/-}$ mice at P0 were subjected to immunofluorescence staining with antibodies to EpCAM. Nuclei were also stained with DAPI. Bar, 20 μm.

obvious in the upper intestine, the duodenum and jejunum (Fig. 1B).

Given the impaired epithelial architecture, we examined whether intestinal stem or progenitor cells are maintained in the mutant mice. In the normal intestine, Ki67-positive (proliferating) cells are localized to the intervillus domains between villi at both embryonic and adult stages (Fig. S6A) (van der Flier et al., 2009). The number of Ki67-positive cells in intervillus domains of EpCAM mutant mice at E18.5 was similar to that in WT animals throughout the intestine (Fig. S6A). Intestinal stem cells, which express *Lgr5*, are also located in intervillus domains (Kim et al., 2012). Again, the number of *Lgr5*-expressing cells in the intestine of mutant mice was similar that in WT controls (Fig. S6B). These results thus suggested that intestinal stem and progenitor cells as well as regulation of their cell cycle are maintained in the intestine of EpCAM mutant mice. Enterocytes, which are positive for β-galactosidase and alkaline phosphatase and (Fig. S7A and B), and goblet cells positive for alcian blue staining (Fig. S7C) were maintained in the intestine of EpCAM mutant mice, suggesting that intestinal cell types are correctly specified in the absence of EpCAM. Apoptosis was not apparent either in the wild-type or EpCAM mutant mice (Fig. S7D).

EpCAM is highly expressed in the developing intestine

In WT mice, *EpCAM* mRNA was detected in the developing gut from E9.5 to E15.5 as well as throughout the intestine, from the duodenum to the colon, at E18.5 (Fig. S8). EpCAM protein was found in villi and intervillus domains and was localized to cell–cell junctions of the intestinal epithelium at E18.5 and at P0 (Figs. 1C and 2A). As expected, EpCAM protein was not detected in the intestine of $EpCAM^{-/-}$ or $EpCAM^{\beta geo/\beta geo}$ mice (Fig. 1C, Fig. S2B). Staining of the intestinal epithelium of WT mice with both antibodies to EpCAM and either those to E-cadherin or those to ZO-1, markers of adherens junctions (AJs) and tight junctions (TJs), respectively, revealed that EpCAM is localized to TJs, AJs and the lateral membranes of the epithelial cells lining the mouse intestines (Fig. 2A).

Claudin proteins are down-regulated in the intestine of EpCAM mutant mice

We next examined the expression of proteins that contribute to cell–cell junctions, including that of claudin-7, which interacts with EpCAM in cultured tumor cells (Kuhn et al., 2007; Ladwein et al., 2005) and is one of the major claudin proteins expressed in the intestine (Fujita et al., 2006) (Fig. 3). In EpCAM mutant embryos at E18.5, however, claudin-7 was down-regulated to undetectable levels in all regions of the intestine examined, including the duodenum, jejunum, ileum, and colon (Fig. 3A, Fig. S3B). Claudin-7 was thus undetectable not only at cell–cell junctions but also in the interior of intestinal cells. Furthermore, whereas claudin-7 is expressed in the epithelium of the normal developing gut at E12.5, E13.5, and E14.5, it was undetectable in the developing gut of the mutant mice at any stage examined (Fig. 3B).

Mice lacking claudin-7 manifest renal salt wasting and chronic dehydration and intestinal anomalies similar to those of EpCAM mutant mice (Ding et al., 2012; Tatum et al., 2010). To examine whether deficiency of claudin-7 alone is responsible for intestinal defects of the EpCAM mutant mouse, we examined the expression of additional junctional proteins, including other claudins as well as AJ and desmosome proteins. Claudin-3 is predominantly expressed in intervillus domains of the developing intestine in WT mice; its abundance was reduced in the intestine of EpCAM mutant mice at P0, however, with this effect being most

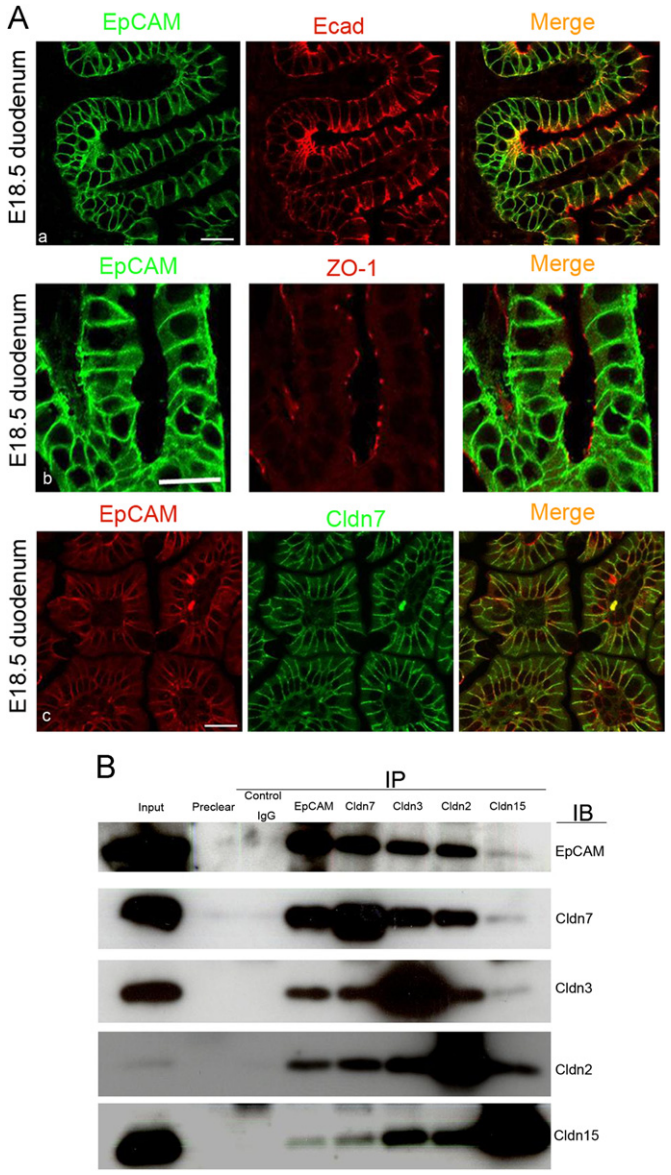

Fig. 2. Colocalization of EpCAM with claudin-7 in the intestine: (A) immunofluorescence staining of the duodenum of E18.5 WT mice with both antibodies to EpCAM and those to either E-cadherin (Ecad, panels a), ZO-1 (panels b), or claudin-7 (Cldn7, panels c). EpCAM localized not only to apical junctions containing E-cadherin and ZO-1 but also to the lateral membrane of neighboring epithelial cells. It also colocalized extensively with claudin-7 along the lateral cell membrane of epithelial cells, indicating that claudin-7 is not a specific TJ marker. Bars, 20 μm. (B) Lysates of the intestine of E18.5 WT mice were subjected to immunoprecipitation (IP) with antibodies to EpCAM, to claudin-7, to claudin-3, to claudin-2, or to claudin-15 or with control rabbit IgG. The resulting precipitates as well as the original lysates (Input) were subjected to immunoblot (IB) analysis with the same antibodies as indicated. "Preclear" lanes represent proteins precipitated from lysates with protein G before incubation with antibodies.

prominent in the duodenum and jejunum (Fig. 4A). Claudin-15, which is normally expressed at TJs of the intestinal epithelium (Fujita et al., 2006), was also down-regulated in the mutant intestine, especially in the duodenum and jejunum (Fig. 4B). Whereas claudin-2 was detected in intestinal villi and intervillus domains of WT mice at P0, it was down-regulated in the mutant intestine (Fig. 4C). The expression of other cell–cell junctional proteins examined, including E-cadherin, β-catenin, and occludin, appeared normal in the intestine of EpCAM mutant mice (Fig. S9). These results thus suggested that deficiency of multiple claudin

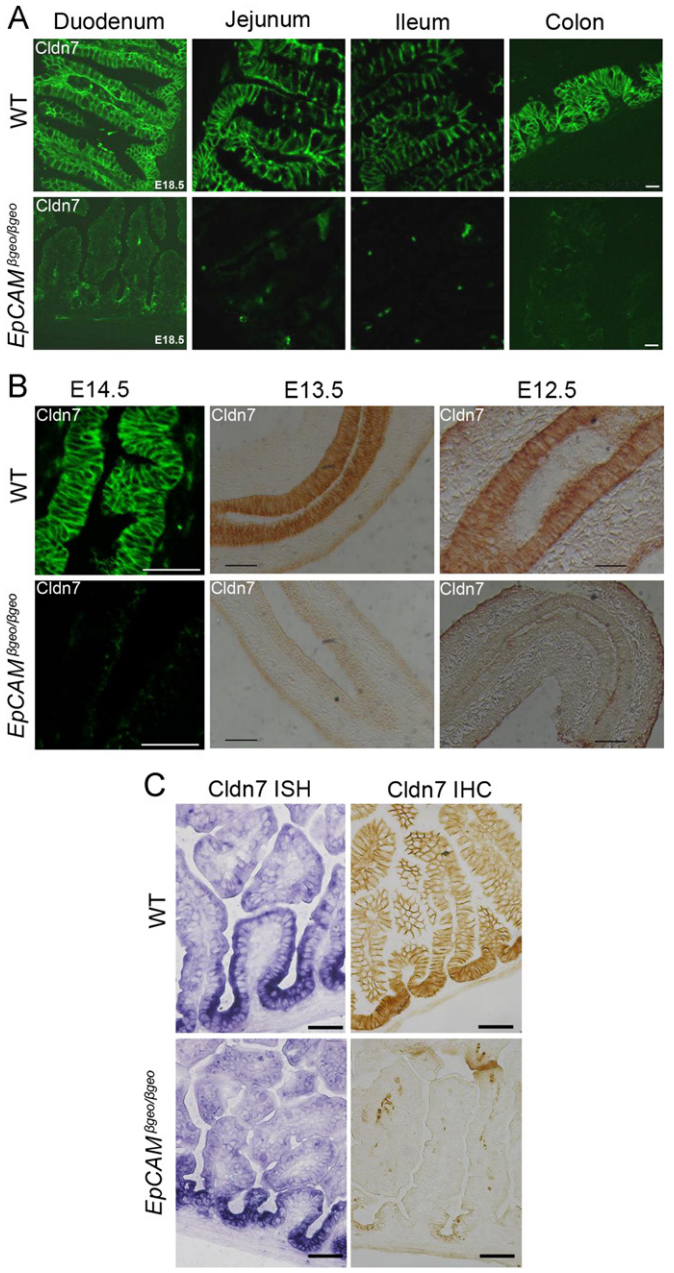

Fig. 3. Down-regulation of claudin-7 in the intestinal epithelium of EpCAM mutant mice: (A) immunofluorescence staining of claudin-7 in the epithelium of the duodenum, jejunum, ileum, and colon of WT and *EpCAM*$^{\beta geo/\beta geo}$ mouse embryos at E18.5. Bars, 20 μm. (B) Immunofluorescence or immunohistochemical staining of claudin-7 in the small intestinal epithelium of WT and *EpCAM*$^{\beta geo/\beta geo}$ mouse embryos at E14.5, E13.5, and E12.5. Bars, 50 μm. (C) In situ hybridization (ISH) analysis of claudin-7 mRNA and immunohistochemical (IHC) analysis of claudin-7 protein in the duodenal epithelium of WT and *EpCAM*$^{\beta geo/\beta geo}$ mouse embryos at E18.5. The sections for the two types of analysis are from the same animals. Bars, 50 μm.

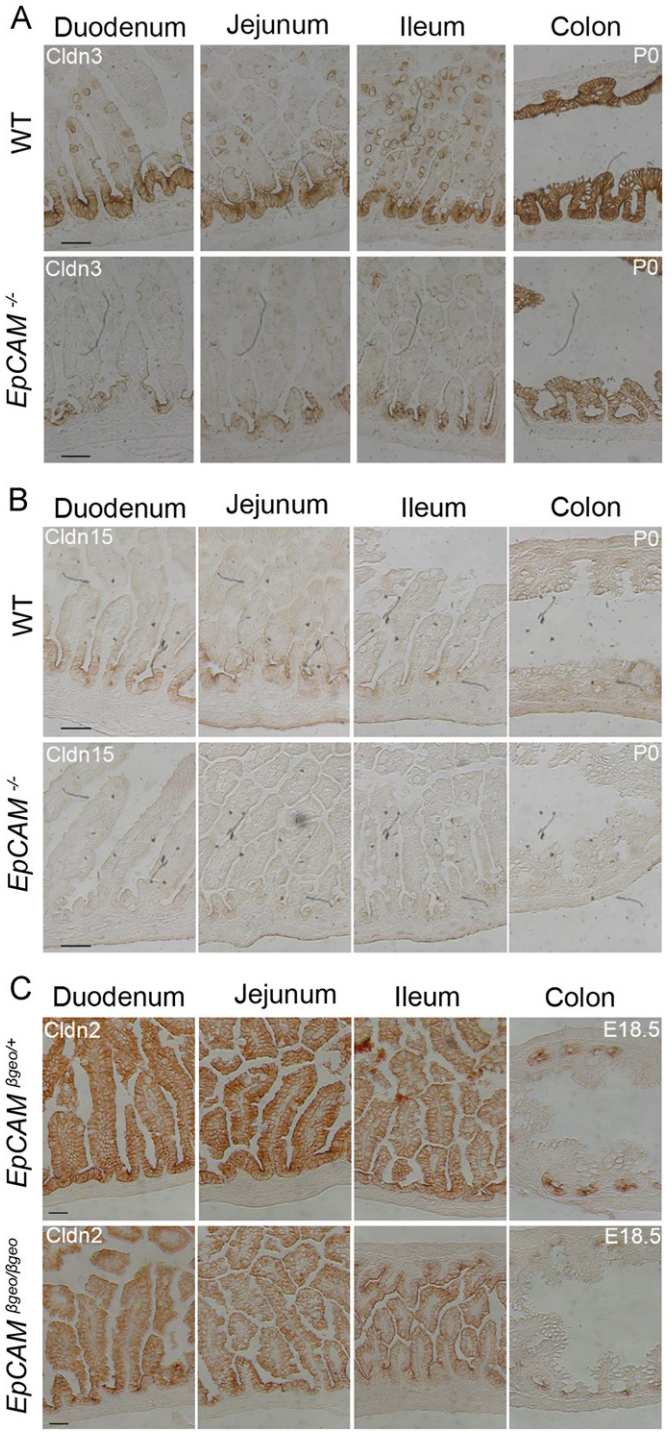

Fig. 4. Down-regulation of claudins 2, 3, and 15 in the intestinal epithelium of EpCAM mutant mice. Immunohistochemical staining of claudin-3 (A), claudin-15 (B) and claudin-2 (C) in the epithelium of the duodenum, jejunum, ileum, and colon of WT and *EpCAM*$^{-/-}$ mouse pups at P0. Claudin-3 and claudin-15 localized to the apical surface of intervillus domains in the intestine of WT mice and were down-regulated in the mutant. Claudin-2 is localized to the apical surface of intestinal villi and intervillus domains in the WT mouse and it is down-regulated in the mutant. Bars, 50 μm.

proteins at cell–cell junctions might be responsible for the intestinal defects of EpCAM mutant mice.

EpCAM interacts with claudins in the intestinal epithelium

Claudin-7, like EpCAM, is abundantly localized to lateral membrane while other claudins localize mainly to apical TJs in the intestinal epithelium. Whereas the abundance of claudin-7 protein was greatly reduced in the intestine of EpCAM mutant mice, that of *claudin-7* mRNA was not (Fig. 3C), suggesting that the down-regulation of claudin-7 expression occurs at a post-transcriptional level. Consistent with previous observations with human tissue and cultured cells (Ladwein et al., 2005), EpCAM and claudin-7 were found to be colocalized at cell–cell junctions of the normal mouse intestinal epithelium (Fig. 2A). We then examined whether EpCAM interacts with claudin-7 in the

intestinal epithelium. Co-immunoprecipitation analysis with the intestine of WT mice revealed that claudin-7 was present in the precipitates obtained with antibodies to EpCAM and vice versa (Fig. 2B). Together, our results thus suggested that EpCAM interacts with claudin-7 to form a complex in the intestinal epithelium, and that localization of claudin-7 to the membrane requires EpCAM. EpCAM also formed a complex with other claudin proteins, including claudins 2, 3, and 15, although the interaction with claudin-15 appeared relatively weak (Fig. 2B).

EST expression data (NCBI) suggested that the genes for EpCAM and claudin-7 are also coexpressed in other organs including lung, pancreas, stomach, and kidney. We therefore examined the expression and localization of claudin-7 in these organs of WT and EpCAM mutant embryos. EpCAM and claudin-7 were indeed found to be coexpressed and colocalized in epithelia of these organs in WT embryos (Fig. 5A). Claudin-7 was not detected in epithelia of the lung, stomach, and pancreas of EpCAM mutant mice, but it was detected in the kidney of EpCAM mutant mice albeit at a reduced level (Fig. 5B).

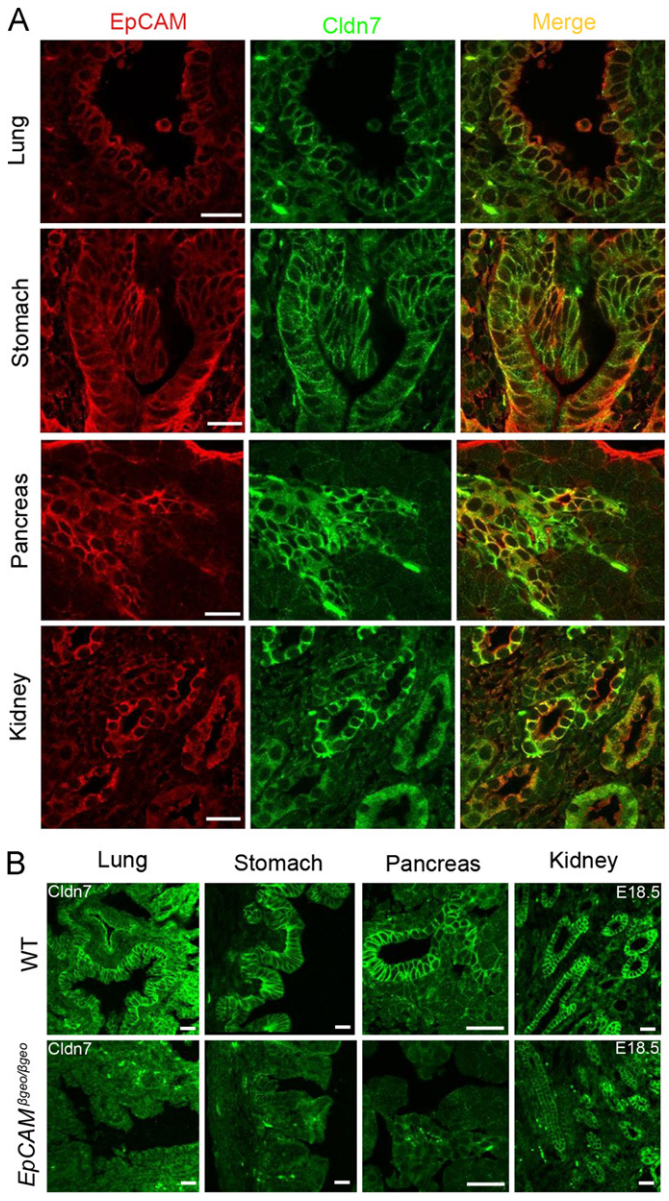

Fig. 5. Down-regulation of claudin-7 in various organs of EpCAM mutant mice: (A) immunofluorescence staining of EpCAM and claudin-7 in lung, stomach, pancreas, and kidney of WT mice at E18.5. The two proteins colocalized in the epithelia of these organs. (B) Immunofluorescence staining of claudin-7 in lung, stomach, pancreas, and kidney of WT and *EpCAM*$^{\beta geo/\beta geo}$ mouse embryos at E18.5. All bars, 20 μm.

Barrier function is impaired in the EpCAM mutant intestinal epithelium

Given that TJs are required for paracellular barrier function (Tsukita and Furuse, 2002; Tsukita et al., 2008), we next examined the barrier function of the intestinal epithelium. Injection of sulfo-NHS-biotin, a probe that physically labels cell membrane proteins, into the intestinal lumen of E18.5 WT embryos revealed that the resulting biotin signal at the basal membrane of epithelial cells in the jejunum was less intense than that at the apical membrane (Fig. 6A). In contrast, similar analysis of the intestine of EpCAM mutant mice showed that the biotin signal at the basal membrane was similar to that at the apical membrane (Fig. 6A). In addition, the intensity of the biotin signal at the lateral membrane of the intestinal epithelium was higher for the mutant mice than for WT mice (Fig. 6A). These results thus suggested that the barrier function of TJs is impaired in the EpCAM mutant animals. Given that the intestine of the mutant mice does not exhibit histological anomalies at E18.5, the impaired barrier function is not likely due to macroscopic structural damage to the intestine. We further evaluated barrier function with a quantitative assay based on a low molecular weight probe, Lucifer yellow. The apical to basal flux as well as the basal to apical flux of this probe were increased in the intestine of EpCAM mutant mice at P3.5 (Fig. 6B). Together, our results suggested that the barrier function of the intestine is impaired in EpCAM mutant mice, most likely as a result of the down-regulation of claudins such as claudins 2, 3, 7, and 15 at TJs.

Claudin-2 and claudin-15 are responsible for paracellular permeability of Na^+ (Tamura et al., 2011). In EpCAM mutant mice in which claudin-2 and claudin-15 are down-regulated (Fig. 4), NaCl-dilution potential was lowered (Fig. 6C). Na^+-selective paracellular permeability was reduced while Cl^--selective permeability remained normal (Fig. 6C), like in the claudin-15 mutant mouse (Tamura et al., 2011).

Structural anomalies of tight junctions in the intestinal epithelium of EpCAM mutant mice

Finally, we examined the structural integrity of cell–cell junctions in the intestinal epithelium by electron microscopy at P1, the stage when the intestine of the mutant mice appeared relatively normal both macroscopically (Fig. 1A) and histologically (Suppl. Fig. 5). Freeze-fracture electron microscopy revealed the branching network of sealing strands of TJs apparent in the intestinal epithelium of WT mice to be scattered and dispersed in that of the mutant mice (Fig. 7A). Analysis of ultrathin sections (Fig. 7B) revealed the presence of cell–cell junctions including TJs, AJs, and desmosomes in the intestinal epithelium of WT mice. In the intestinal epithelium of EpCAM mutant mice, however, TJs expanded and appeared markedly dispersed and less well organized (Fig. 7B). On the other hand, the structure of AJs appeared to be normal in the mutant animals (Fig. 7A). These structural anomalies of TJs likely account for the impaired barrier function of the mutant intestinal epithelium (Fig. 6).

Discussion

We have uncovered a role for EpCAM in formation of functional TJs of the intestinal epithelium. TJs form a barrier that separates the apical from the basolateral membrane of the

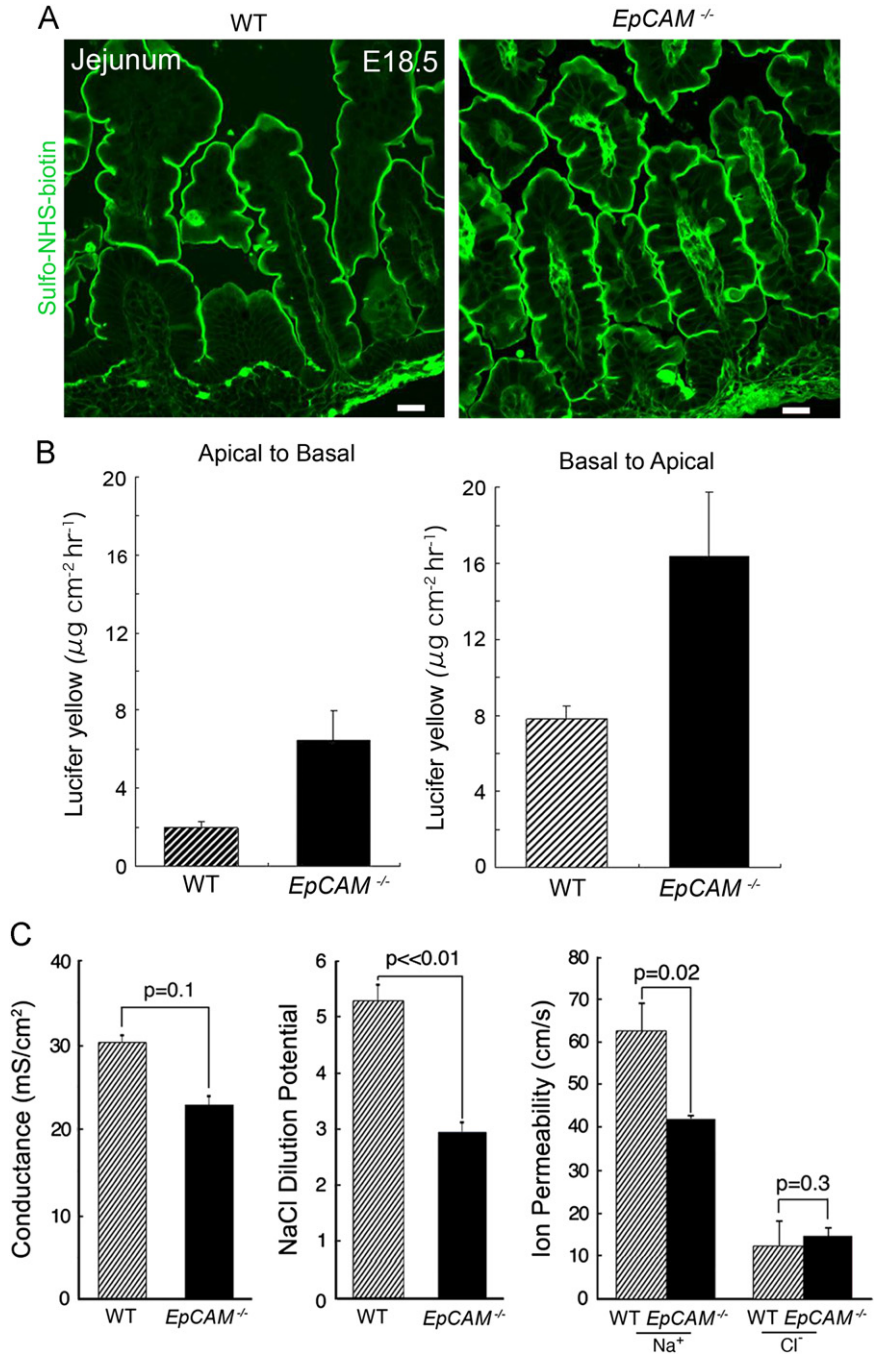

Fig. 6. Impaired barrier function of the intestinal epithelium in EpCAM mutant mice: (A) fluorescence staining of proteins labeled with sulfo-NHS-biotin in the jejunum after injection of the probe into the lumen of the intestine of WT or *EpCAM*$^{-/-}$ embryos at E18.5. Whereas the biotin signal at the basal membrane is less intense than that at the apical membrane for the WT intestine, it is similar to that at the apical membrane for the mutant intestine. The biotin signal at the lateral membrane of the epithelium is also more intense for the mutant embryo than for the WT embryo. Bars, 20 μm. (B) Measurement of the flux of Lucifer yellow from the apical to basal side and from the basal to apical side of the jejunum isolated from WT or *EpCAM*$^{-/-}$ mouse pups at P3.5. Data are means ± SEM from 10 (apical to basal) or 8 (basal to apical) independent experiments. (C) Electrophysiologic analyses were performed as described previously (Tamura et al., 2011). Analyses of the ionic conductances across the small intestine of WT or *EpCAM*$^{-/-}$ mice at P3.5 show that transepithelial conductance remains relatively normal in the *EpCAM*$^{-/-}$ mouse (left panel). Transepithelial NaCl dilution potentials across the small intestine of WT or *EpCAM*$^{-/-}$ mice at P3.5 suggest that permeability for NaCl is significantly reduced in the *EpCAM*$^{-/-}$ mouse (the middle panel). Na^+ paracellular permeability is reduced while Cl^- paracellular permeability does not change in the *EpCAM*$^{-/-}$ mouse (right panel).

epithelium, allowing the selective passage of ions and solutes (Van Campenhout et al., 2011). Members of the claudin family, which includes at least 27 proteins in human and mouse (Mineta et al., 2011; Tsukita and Furuse, 2002; Tsukita et al., 2008; Van Itallie and Anderson, 2006; Yu and Turner, 2008), are essential components of TJs (Angelow et al., 2008). They have been shown to determine not only the barrier function but also the paracellular permeability of epithelial cell sheets in culture (Colegio et al., 2002; Furuse and Tsukita, 2006; Van Itallie and Anderson, 2006). The combined down-regulation of claudins-2, 3, 7, and 15 observed in the intestinal epithelium of EpCAM mutant mice in the present study might thus account for the impaired barrier function in the intestine of these animals. In fact, a recent study (Ding et al., 2012) reported that mutant mouse lacking claudin-7 manifests intestinal defects similar to those of the EpCAM mutant mice. With the barrier function impaired, large molecules such as

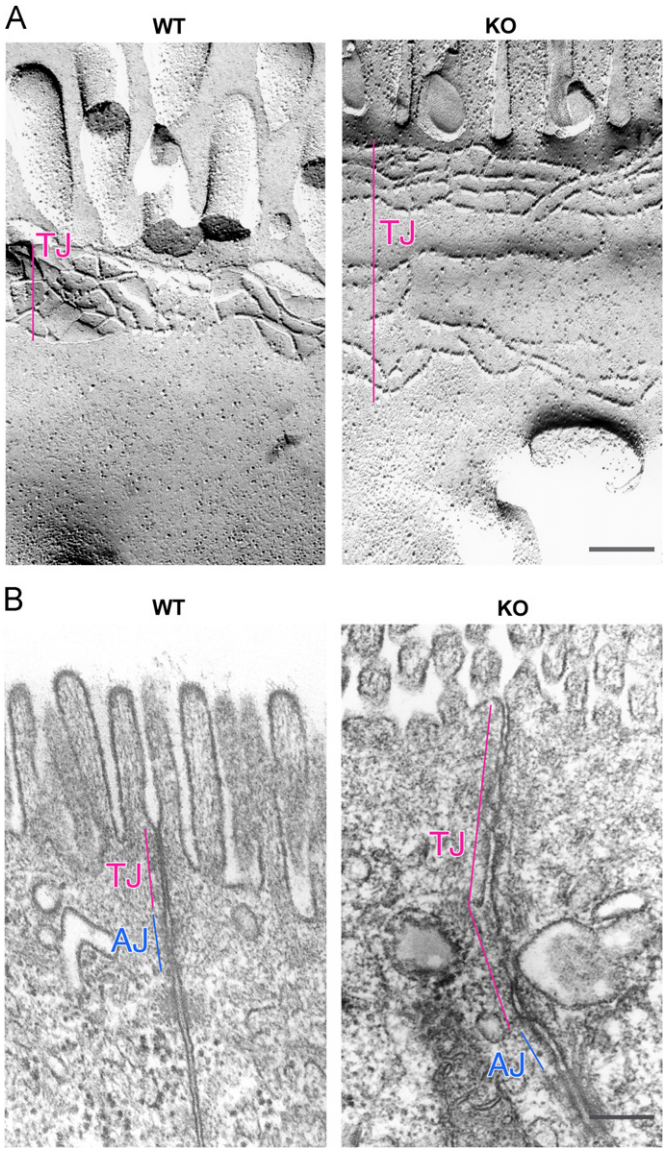

Fig. 7. Aberrant structure of tight junctions in the intestinal epithelium of EpCAM mutant mice: (A) freeze-fracture electron micrographs showing TJ strands in the jejunum of WT and *EpCAM*$^{\beta geo/\beta geo}$ (KO) mice at P1. Bar, 200 nm. (B) Transmission electron micrographs of ultrathin sections showing TJs (pink) and AJs (blue) in the jejunal epithelium of WT and *EpCAM*$^{\beta geo/\beta geo}$ (KO) mouse pups at P1. Bar, 200 nm.

proteases may have penetrated the mutant intestinal epithelium, which may be the reason for the intestinal erosion found in the *EpCAM* mutant mouse. In this regard, it is interesting to note that the intestinal defects of EpCAM mutant mice were more severe in the upper parts of the intestine (Fig. 1B), where proteases are more abundant.

Our results suggest that EpCAM contributes to the formation of a functional barrier in the intestinal epithelium by recruiting claudins to TJs. An EpCAM mutant mouse line generated previously did not survive beyond E12.5 and manifested embryonic mortality as a result of placental defects (Nagao et al., 2009). Although a small portion of our lines of EpCAM mutant mice may be embryonic lethal, we did not observe a substantial loss of mutant embryos during pregnancy. Although the two studies adopted different targeting strategies, it is likely that they both resulted in the generation of functionally null alleles. The genetic background of the mice was also 129/C57B6 in both studies. The reason for the discrepancy in embryonic lethality therefore remains unknown.

EpCAM is expressed in embryonic and somatic stem cells and is implicated in pluripotency. Although our EpCAM mutant mice appear to develop normally until birth, a maternal contribution of EpCAM might have prevented early embryonic death of the mutant animals. A minor proportion (3/50, 6%) of the mutant mice survives until adulthood, with both males and females being fertile. EpCAM therefore appears to be dispensable for germ cell formation, even though it is highly expressed in primordial germ cells (Fig. S1B). Such EpCAM mutant mice that survive until adulthood should prove useful for investigation of the possible role of EpCAM in maintenance of somatic stem cells such as those in the liver (Okabe et al., 2009; Schmelzer et al., 2006) as well as that of cancer stem cells.

We found that EpCAM and claudin-7 are colocalized not only at TJs but also at the lateral membrane of intestinal epithelial cells. Electron microscopy of ultrathin sections revealed that TJs are structurally abnormal in the intestinal epithelium of EpCAM mutant mice. However, AJs appear structurally normal and accordingly the level of membrane-associated E-cadherin was maintained in the mutant. These observations suggest that EpCAM may be specifically required to form functional TJs by recruiting claudins to TJ. Down-regulation of TJ-localized claudins such as claudin 2, 3, 15 might have made major contribution to the specific defects of TJs. In general, formation of TJs and that of AJs appear to affect each other since AJs and TJs are interconnected. Indeed, AJs have been found to be necessary for the establishment of TJs (Gladden et al., 2010), and some TJ proteins are mislocalized and functional TJs are not formed in the absence of α-catenin or cadherin (Tinkle et al., 2008; Tunggal et al., 2005; Vasioukhin et al., 2001). Under certain conditions, however, AJs may be formed normally even when structural integrity of TJ is compromised.

Claudin-7 was the most extensively down-regulated claudin in the intestinal epithelium of EpCAM mutant mice. However, the combined down-regulation of multiple claudins may thus underlie the intestinal defects of EpCAM mutant mice. Claudin-7 localizes to TJs and the lateral membrane of epithelial cells in many mouse and human tissues (Ladwein et al., 2005; Tatum et al., 2010). What then is the mechanism by which claudin-7 is down-regulated to undetectable levels in the intestine of EpCAM mutant mice? Given that the abundance of claudin-7 mRNA was maintained in the intestine of these animals, the reduction in the amount of claudin-7 protein appears to occur at a posttranscriptional step. Previous studies (Kuhn et al., 2007; Ladwein et al., 2005) and our present results suggest that EpCAM associates with claudin-7 in various cultured cells and tissues. Interaction with EpCAM may result in the recruitment of claudin-7 to AJs and TJs, such that, in the absence of EpCAM, claudin-7 becomes mislocalized and susceptible to degradation by the ubiquitin-proteasome system. However, treatment of duodenum explants from EpCAM mutant mice with MG132 (a proteasome inhibitor) did not increase the level of claudin-7 (Fig. S10), suggesting claudin-7 may be degraded by some other mechanism such as the one involving the lysosome. Whereas claudin-7 was also not detected in the lung, stomach, and pancreas of EpCAM mutant mice, it was still detected in the kidney epithelium, albeit at reduced levels. The kidney epithelium may thus express an EpCAM-like protein that associates with claudin-7. Tacstd2 is a candidate for such an EpCAM-like molecule, given that it is not only structurally related to EpCAM but it also interacts with claudin-1 and claudin-7 in human tissues and cultured cells and its knockdown reduces the levels of these claudins (Nakatsukasa et al., 2010).

In addition to claudin-7, the levels of claudins 2, 3, and 15 were also reduced in the intestine of EpCAM mutant mice. EpCAM

may therefore directly interact with a variety of claudins and recruit them to cell–cell junctions including AJs and TJs. Claudin molecules associate with each other in a heterotypic as well as homotypic manner in cultured cells (Daugherty et al., 2007; Furuse et al., 1999; Piontek et al., 2008). We found that claudins 2, 3, 7, and 15 were coprecipitated with each other from intestinal lysates. However, as mentioned above, the distribution and expression level of claudins 2, 3, 4, and 8 in the kidney were not affected in claudin-7 knockout mice (Tatum et al., 2010). The precise manner of interaction between EpCAM and various claudins therefore remains to be determined.

Acknowledgments

We thank Y. Ikawa and S. Oishi for technical assistance. This work was supported by a grant from Core Research for Evolutional Science and Technology (CREST) of the Japan Science and Technology Corporation and a Grant-in-Aid from the Ministry of Education, Culture, Sports, Science, and Technology of Japan (to H.H.)

Appendix A. Supporting information

Supplementary data associated with this article can be found in the online version at http://dx.doi.org/10.1016/j.ydbio.2012.07.005.

References

Angelow, S., Ahlstrom, R., Yu, A.S., 2008. Biology of claudins. Am. J. Physiol. Renal Physiol. 295, F867–F876.

Colegio, O.R., Van Itallie, C.M., McCrea, H.J., Rahner, C., Anderson, J.M., 2002. Claudins create charge-selective channels in the paracellular pathway between epithelial cells. Am. J. Physiol. Cell Physiol. 283, C142–C147.

Dalerba, P., Dylla, S.J., Park, I.K., Liu, R., Wang, X., Cho, R.W., Hoey, T., Gurney, A., Huang, E.H., Simeone, D.M., Shelton, A.A., Parmiani, G., Castelli, C., Clarke, M.F., 2007. Phenotypic characterization of human colorectal cancer stem cells. Proc. Natl. Acad. Sci. USA 104, 10158–10163.

Daugherty, B.L., Ward, C., Smith, T., Ritzenthaler, J.D., Koval, M., 2007. Regulation of heterotypic claudin compatibility. J. Biol. Chem. 282, 30005–30013.

de Boer, C.J., van Krieken, J.H., Janssen-van Rhijn, C.M., Litvinov, S.V., 1999. Expression of Ep-CAM in normal, regenerating, metaplastic, and neoplastic liver. J. Pathol. 188, 201–206.

Ding, L., Lu, Z., Foreman, O., Tatum, R., Lu, Q., Renegar, R., Cao, J., Chen, Y.H., 2012. Inflammation and disruption of the mucosal architecture in claudin-7-deficient mice. Gastroenterology. 142, 305–15.

Fujita, H., Chiba, H., Yokozaki, H., Sakai, N., Sugimoto, K., Wada, T., Kojima, T., Yamashita, T., Sawada, N., 2006. Differential expression and subcellular localization of claudin-7, -8, -12, -13, and -15 along the mouse intestine. J. Histochem. Cytochem. 54, 933–944.

Furuse, M., Sasaki, H., Tsukita, S., 1999. Manner of interaction of heterogeneous claudin species within and between tight junction strands. J. Cell Biol. 147, 891–903.

Furuse, M., Tsukita, S., 2006. Claudins in occluding junctions of humans and flies. Trends Cell Biol. 16, 181–188.

Gladden, A.B., Hebert, A.M., Schneeberger, E.E., McClatchey, A.I., 2010. The NF2 tumor suppressor, Merlin, regulates epidermal development through the establishment of a junctional polarity complex. Dev. Cell. 19, 727–739.

Gonzalez, B., Denzel, S., Mack, B., Conrad, M., Gires, O., 2009. EpCAM is involved in maintenance of the murine embryonic stem cell phenotype. Stem Cells 27, 1782–1791.

Kim, T.H., Escudero, S., Shivdasani, R.A., 2012. Intact function of Lgr5 receptor-expressing intestinal stem cells in the absence of Paneth cells. Proc. Natl. Acad. Sci. USA 109, 3932–3937.

Kuhn, S., Koch, M., Nubel, T., Ladwein, M., Antolovic, D., Klingbeil, P., Hildebrand, D., Moldenhauer, G., Langbein, L., Franke, W.W., Weitz, J., Zoller, M., 2007. A complex of EpCAM, claudin-7, CD44 variant isoforms, and tetraspanins promotes colorectal cancer progression. Mol. Cancer Res. 5, 553–567.

Ladwein, M., Pape, U.F., Schmidt, D.S., Schnolzer, M., Fiedler, S., Langbein, L., Franke, W.W., Moldenhauer, G., Zoller, M., 2005. The cell–cell adhesion molecule EpCAM interacts directly with the tight junction protein claudin-7. Exp. Cell Res. 309, 345–357.

Litvinov, S.V., Balzar, M., Winter, M.J., Bakker, H.A., Briaire-de Bruijn, I.H., Prins, F., Fleuren, G.J., Warnaar, S.O., 1997. Epithelial cell adhesion molecule (Ep-CAM) modulates cell–cell interactions mediated by classic cadherins. J. Cell Biol. 139, 1337–1348.

Litvinov, S.V., Velders, M.P., Bakker, H.A., Fleuren, G.J., Warnaar, S.O., 1994. Ep–CAM: a human epithelial antigen is a homophilic cell–cell adhesion molecule. J. Cell Biol. 125, 437–446.

Lu, T.Y., Lu, R.M., Liao, M.Y., Yu, J., Chung, C.H., Kao, C.F., Wu, H.C., 2010. Epithelial cell adhesion molecule regulation is associated with the maintenance of the undifferentiated phenotype of human embryonic stem cells. J. Biol. Chem. 285, 8719–8732.

Maetzel, D., Denzel, S., Mack, B., Canis, M., Went, P., Benk, M., Kieu, C., Papior, P., Baeuerle, P.A., Munz, M., Gires, O., 2009. Nuclear signalling by tumour-associated antigen EpCAM. Nat. Cell Biol. 11, 162–171.

Maghzal, N., Vogt, E., Reintsch, W., Fraser, J.S., Fagotto, F., 2010. The tumor-associated EpCAM regulates morphogenetic movements through intracellular signaling. J. Cell Biol. 191, 645–659.

Mineta, K., Yamamoto, Y., Yamazaki, Y., Tanaka, H., Tada, Y., Saito, K., Tamura, A., Igarashi, M., Endo, T., Takeuchi, K., Tsukita, S., 2011. Predicted expansion of the claudin multigene family. FEBS Lett. 585, 606–612.

Nagao, K., Zhu, J., Heneghan, M.B., Hanson, J.C., Morasso, M.I., Tessarollo, L., Mackem, S., Udey, M.C., 2009. Abnormal placental development and early embryonic lethality in EpCAM-null mice. PLoS One 4, e8543.

Nakatsukasa, M., Kawasaki, S., Yamasaki, K., Fukuoka, H., Matsuda, A., Tsujikawa, M., Tanioka, H., Nagata-Takaoka, M., Hamuro, J., Kinoshita, S., 2010. Tumor-associated calcium signal transducer 2 is required for the proper subcellular localization of claudin 1 and 7: implications in the pathogenesis of gelatinous drop-like corneal dystrophy. Am. J. Pathol. 177, 1344–1355.

Okabe, M., Tsukahara, Y., Tanaka, M., Suzuki, K., Saito, S., Kamiya, Y., Tsujimura, T., Nakamura, K., Miyajima, A., 2009. Potential hepatic stem cells reside in EpCAM+ cells of normal and injured mouse liver. Development 136, 1951–1960.

Piontek, J., Winkler, L., Wolburg, H., Muller, S.L., Zuleger, N., Piehl, C., Wiesner, B., Krause, G., Blasig, I.E., 2008. Formation of tight junction: determinants of homophilic interaction between classic claudins. FASEB J. 22, 146–158.

Saijoh, Y., Fujii, H., Meno, C., Sato, M., Hirota, Y., Nagamatsu, S., Ikeda, M., Hamada, H., 1996. Identification of putative downstream genes of Oct-3, a pluripotent cell-specific transcription factor. Genes Cells 1, 239–252.

Schmelzer, E., Wauthier, E., Reid, L.M., 2006. The phenotypes of pluripotent human hepatic progenitors. Stem Cells 24, 1852–1858.

Schmelzer, E., Zhang, L., Bruce, A., Wauthier, E., Ludlow, J., Yao, H.L., Moss, N., Melhem, A., McClelland, R., Turner, W., Kulik, M., Sherwood, S., Tallheden, T., Cheng, N., Furth, M.E., Reid, L.M., 2007. Human hepatic stem cells from fetal and postnatal donors. J. Exp. Med. 204, 1973–1987.

Scholer, H.R., Ruppert, S., Suzuki, N., Chowdhury, K., Gruss, P., 1990. New type of POU domain in germ line-specific protein Oct-4. Nature 344, 435–439.

Shimazaki, T., Okazawa, H., Fujii, H., Ikeda, M., Tamai, K., McKay, R.D., Muramatsu, M., Hamada, H., 1993. Hybrid cell extinction and re-expression of Oct-3 function correlates with differentiation potential. EMBO J. 12, 4489–4498.

Slanchev, K., Carney, T.J., Stemmler, M.P., Koschorz, B., Amsterdam, A., Schwarz, H., Hammerschmidt, M., 2009. The epithelial cell adhesion molecule EpCAM is required for epithelial morphogenesis and integrity during zebrafish epiboly and skin development. PLoS Genet. 5, e1000563.

Tamura, A., Hayashi, H., Imasato, M., Yamazaki, Y., Hagiwara, A., Wada, M., Noda, T., Watanabe, M., Suzuki, Y., Tsukita, S., 2011. Loss of claudin-15, but not claudin-2, causes Na+ deficiency and glucose malabsorption in mouse small intestine. Gastroenterology 140, 913–923.

Tamura, A., Kitano, Y., Hata, M., Katsuno, T., Moriwaki, K., Sasaki, H., Hayashi, H., Suzuki, Y., Noda, T., Furuse, M., Tsukita, S., 2008. Megaintestine in claudin-15-deficient mice. Gastroenterology 134, 523–534.

Tanaka, M., Okabe, M., Suzuki, K., Kamiya, Y., Tsukahara, Y., Saito, S., Miyajima, A., 2009. Mouse hepatoblasts at distinct developmental stages are characterized by expression of EpCAM and DLK1: drastic change of EpCAM expression during liver development. Mech. Dev. 126, 665–676.

Tatum, R., Zhang, Y., Salleng, K., Lu, Z., Lin, J.J., Lu, Q., Jeansonne, B.G., Ding, L., Chen, Y.H., 2010. Renal salt wasting and chronic dehydration in claudin-7-deficient mice. Am. J. Physiol. Ren. Physiol. 298, F24–F34.

Tinkle, C.L., Pasolli, H.A., Stokes, N., Fuchs, E., 2008. New insights into cadherin function in epidermal sheet formation and maintenance of tissue integrity. Proc. Natl. Acad. Sci. USA 105, 15405–15410.

Trzpis, M., McLaughlin, P.M., de Leij, L.M., Harmsen, M.C., 2007. Epithelial cell adhesion molecule: more than a carcinoma marker and adhesion molecule. Am. J. Pathol. 171, 386–395.

Tsukita, S., Furuse, M., 2002. Claudin-based barrier in simple and stratified cellular sheets. Curr. Opin. Cell Biol. 14, 531–536.

Tsukita, S., Furuse, M., Itoh, M., 2001. Multifunctional strands in tight junctions. Nat. Rev. Mol. Cell Biol. 2, 285–293.

Tsukita, S., Yamazaki, Y., Katsuno, T., Tamura, A., 2008. Tight junction-based epithelial microenvironment and cell proliferation. Oncogene 27, 6930–6938.

Tunggal, J.A., Helfrich, I., Schmitz, A., Schwarz, H., Gunzel, D., Fromm, M., Kemler, R., Krieg, T., Niessen, C.M., 2005. E-cadherin is essential for in vivo epidermal barrier function by regulating tight junctions. EMBO J. 24, 1146–1156.

Van Campenhout, C.A., Eitelhuber, A., Gloeckner, C.J., Giallonardo, P., Gegg, M., Oller, H., Grant, S.G., Krappmann, D., Ueffing, M., Lickert, H., 2011. Dlg3 trafficking and apical tight junction formation is regulated by nedd4 and nedd4-2 e3 ubiquitin ligases. Dev. Cell 21, 479–491.

van der Flier, L.G., van Gijn, M.E., Hatzis, P., Kujala, P., Haegebarth, A., Stange, D.E., Begthel, H., van den Born, M., Guryev, V., Oving, I., van Es, J.H., Barker, N.,

Peters, X.W., van de Wetering, M., Clevers, H., 2009. Transcription factor achaete scute-like 2 controls intestinal stem cell fate. Cell 136, 903–912.
Van Itallie, C.M., Anderson, J.M., 2006. Claudins and epithelial paracellular transport. Annu. Rev. Physiol. 68, 403–429.
Vasioukhin, V., Bauer, C., Degenstein, L., Wise, B., Fuchs, E., 2001. Hyperproliferation and defects in epithelial polarity upon conditional ablation of alpha-catenin in skin. Cell 104, 605–617.
Winter, M.J., Nagtegaal, I.D., van Krieken, J.H., Litvinov, S.V., 2003. The epithelial cell adhesion molecule (Ep-CAM) as a morphoregulatory molecule is a tool in surgical pathology. Am. J. Pathol. 163, 2139–2148.
Wilkinson, D.G., 1992. Whole mount in situ hybridisation of vertebrate embryos. In: Wilkinson, D.G., (Eds.), In Situ Hybridisation: A Practical Approach. IRL Press, Oxford, pp.75–83.
Yamashita, T., Ji, J., Budhu, A., Forgues, M., Yang, W., Wang, H.Y., Jia, H., Ye, Q., Qin, L.X., Wauthier, E., Reid, L.M., Minato, H., Honda, M., Kaneko, S., Tang, Z.Y., Wang, X.W., 2009. EpCAM-positive hepatocellular carcinoma cells are tumor-initiating cells with stem/progenitor cell features. Gastroenterology 136, 1012–1024.
Yu, D., Turner, J.R., 2008. Stimulus-induced reorganization of tight junction structure: the role of membrane traffic. Biochim. Biophys. Acta 1778, 709–716.